doi:10.1093/brain/awt128 Brain 2013: 136; 2147–2158 | 2147

BRAIN
A JOURNAL OF NEUROLOGY

Progressive sleep and electroencephalogram changes in mice carrying the Huntington's disease mutation

Sandor Kantor,[1] Lajos Szabo,[1] Janos Varga,[1,2] Marc Cuesta[1,3] and A. Jennifer Morton[1]

1 Department of Physiology, Development and Neuroscience, University of Cambridge, Cambridge, CB2 3DY, UK
2 Department of Behavioural Neurobiology, Institute of Experimental Medicine, Hungarian Academy of Sciences, Budapest, H-1083, Hungary
3 Centre for Study and Treatment of Circadian Rhythms, Douglas Mental Health University Institute, Montreal, Quebec, H4H 1R3, Canada

Correspondence to: A. Jennifer Morton,
Department of Physiology,
Development and Neuroscience,
University of Cambridge,
Downing Street,
Cambridge CB2 3DY,
UK
E-mail: ajm41@cam.ac.uk

Sleep disturbances in Huntington's disease may be deleterious to the cognitive performance, affective behaviour, and general well-being of patients, but a comprehensive description of the progression of changes in sleep and electroencephalogram in Huntington's disease has never been conducted. Here we studied sleep and electroencephalogram disturbances in a transgenic mouse model of Huntington's disease (R6/2 mice). We implanted 10 R6/2 mice and five wild-type littermates with electromyography electrodes, frontofrontal and frontoparietal electroencephalogram electrodes and then recorded sleep/wake behaviour at presymptomatic, symptomatic and late stages of the disease. In addition to sleep–wake scoring, we performed a spectral analysis of the sleep electroencephalogram. We found that sleep and electroencephalogram were already significantly disrupted in R6/2 mice at 9 weeks of age (presymptomatic stage). By the time they were symptomatic, R6/2 mice were unable to maintain long periods of wakefulness and had an increased propensity for rapid eye movement sleep. In addition, the peak frequency of theta rhythm was shifted progressively from 7 Hz to 6 Hz during rapid eye movement sleep, whereas slow wave activity decreased gradually during non-rapid eye movement sleep. Finally, as the disease progressed, an abnormal electroencephalogram gamma activity (30–40 Hz) emerged in R6/2 mice irrespective of sleep states. This is reminiscent of the increased gamma power described in schizophrenic patients during sleep and events of psychosis. Gaining a better understanding of sleep and electroencephalogram changes in patients with Huntington's disease should be a priority, since it will enable clinicians to initiate appropriate investigations and to instigate treatments that could dramatically improve patients' quality of life.

Keywords: EEG; R6/2 mice; REM sleep theta; slow wave activity; gamma activity

Introduction

Huntington's disease is best known as a movement disorder, but non-motor symptoms, such as cognitive impairment, irritability, depression and other psychiatric symptoms, are also present in patients with Huntington's disease. Abnormalities in circadian rhythmicity have been demonstrated in both human patients (Wiegand *et al.*, 1991*a*; Morton *et al.*, 2005; Videnovic *et al.*,

Received January 24, 2013. Revised March 14, 2013. Accepted April 2, 2013

2009; Aziz *et al.*, 2010) and in rodent models of Huntington's disease (Morton *et al.*, 2005; Bode *et al.*, 2009; Kudo *et al.*, 2011). Patients with Huntington's disease show abnormal day–night activity patterns, although they do not typically complain about sleep disturbance or show excessive daytime sleepiness when standard sleep questionnaires are used (Morton *et al.*, 2005; Goodman *et al.*, 2011). Nevertheless, in mouse model of Huntington's disease, circadian abnormalities have now been confirmed by three different laboratories (Morton *et al.*, 2005; Rudenko *et al.*, 2009; Kudo *et al.*, 2011), with R6/2 transgenic mice showing a progressive disintegration of the rest–activity rhythm that mirrors circadian disturbances observed in patients with Huntington's disease (Morton *et al.*, 2005; Kudo *et al.*, 2011).

In addition to circadian abnormalities, sleep and electroencephalogram (EEG) are frequently disturbed in neurodegenerative diseases, with the nature of the impairments in different diseases showing a number of similarities (Petit *et al.*, 2004). Sleep disruption is likely to be a widespread problem in patients with Huntington's disease, because when sleep was assessed by a Huntington's disease-targeted questionnaire, almost all patients acknowledged having sleep problems that were rated by the majority of patients as being either a 'very' or a 'moderately' important problem (Goodman *et al.*, 2010). Despite this, few well-controlled polysomnographic studies have been conducted in patients with Huntington's disease, and the results of those that have been done are inconsistent (Nguyen *et al.*, 2010; Morton, 2013).

Study of sleep and EEG could be a valuable tool for investigating Huntington's disease, since early and progressive abnormalities could serve as biological markers of the disease. Here we analysed the sleep and EEG changes in R6/2 mice, one of the best characterized animal models of Huntington's disease. We found that sleep and EEG are already significantly disrupted in R6/2 mice at the earliest presymptomatic stage of the disease that we measured.

Materials and methods

Animals and housing conditions

All experiments were conducted under the authority of the United Kingdom Animals (Scientific Procedures) Act 1986. Wild-type and R6/2 mice were taken from a colony established at the University of Cambridge (CBAxC57/BL6 background). Genotyping and repeat length measurement were performed by Laragen. Genotyping was performed by PCR from tail snips taken at 3 weeks of age and CAG repeat lengths were measured by GeneMapper software. In total, six male and eight female wild-type mice plus 10 male and eight female R6/2 mice from both sexes were pooled. Successful recordings were not achieved for all mice at every time point due to data logging failures (early termination of data collection). Because we wanted to compare longitudinal changes, here we have presented only those data that were recorded from mice from which successful recordings were made at each time point (presymptomatic, symptomatic, and late stage of the disease). Thus the data from five wild-type mice (three male and two female), and 10 R6/2 mice (seven male and three female) were used for comparisons. These 10 R6/2 mice had a mean CAG repeat length of 253 ± 1.

Surgery and electroencephalogram/electromyogram recordings

Mice were anaesthetized with isoflurane (1.5–2%) and placed in a stereotaxic apparatus. We implanted each mouse with EEG electrodes by placing gold-plated stainless steel screw electrodes epidurally over the left and right frontal cortex (1.5 mm lateral and 1.0 mm anterior to bregma) and left parietal cortex (1.5 mm lateral and 1.0 mm anterior to lambda) for frontofrontal and frontoparietal EEG recordings. Electromyogram (EMG) signals were acquired by a pair of stainless steel spring wires (Plastics One Inc) inserted into the neck extensor muscles (Kantor *et al.*, 2009). Before implantation, each screw was soldered to a soft insulated stainless steel wire, and all cables were connected to a single common seven-pin connector, compatible with the logging device. Cables and the connector were all fixed to the skull with dental cement. The connector was mounted carefully at an angle suitable for the data-logging device.

After surgery, we housed the mice in individual recording cages (with food and water available *ad libitum*) within sound-attenuated chambers with a 12:12 h light-dark cycle (30 lx daylight-type fluorescent tubes with lights on at 06:00), constant temperature ($22 \pm 1^{\circ}C$) and humidity ($55 \pm 10\%$). After a recovery period of 7–10 days, we connected a 'dummy' logging device (a plastic device of weight and form similar to the data-logging device) to the mice. After mice acclimated to the recording conditions for 3–4 days, we replaced the 'dummy' device with the data-logging device (NeuroLogger, TSE Systems GmbH) and recorded EEG and EMG for 24 h. These loggers have a weight of 2.8 g including batteries and data storage capacity up to 512 MB (Etholm *et al.*, 2010). Finally, the loggers were removed from the mice and the data were downloaded by the use of a docking station connected to a PC by a USB cable.

Data analysis and statistics

The EEG/EMG signals were digitized at 256 Hz, digitally filtered (EEG: 1–60 Hz, EMG: 5–60 Hz), and semi-automatically scored as wake, non-REM sleep, or REM sleep in 10 s epochs using SleepSign (Kissei Comtec). Experienced scorers visually inspected these preliminary scorings and made corrections when appropriate. Scorers were blinded to genotype, although at late stages, EEG 'signatures' of Huntington's disease became so apparent in symptomatic R6/2 mice that an experienced scorer could easily identify the correct genotype of the mice based solely on these EEG changes. We then measured the duration of bouts, counted the number of bouts, and calculated the percentage of time spent in each behavioural state.

To compare the ability of mice to maintain wakefulness, we analysed the distribution of wake as a function of bout length. We separated all wake bouts into one of eight bins (<30, 40–70, 80–150, 160–310, 320–630, 640–1270, 1280–2550 and >2560 s) according to length (Trachsel *et al.*, 1991; Franken *et al.*, 1999; Mochizuki *et al.*, 2004). The percentage of wake occurring in each bin was measured and presented in a time-weighted frequency histogram.

To measure the propensity for REM sleep, we analysed REM sleep bout numbers and durations, and the probability of transitioning into REM sleep from non-REM sleep. To analyse the probability of transitioning into REM sleep as a function of non-REM sleep bout length, we first calculated the absolute probability of transitioning from non-REM into REM sleep by counting the incidence of REM sleep

after each 10 s epoch of non-REM sleep. Then we calculated the weighted average probability for non-REM sleep bins of increasing duration (<60, 60–120, 120–180, 180–240, 240–300, 300–360 and >360 s). The sleep cycle was defined as beginning at the onset of non-REM sleep and as ending at the offset of REM sleep, allowing for brief awakenings of no longer than 10 s. Cycles were excluded from analysis if (i) they lacked REM sleep; (ii) the REM sleep episode was only one epoch long (10 s), followed by non-REM sleep; or (iii) the non-REM sleep episode before REM sleep was shorter than 30 s (Kantor *et al.*, 2009).

EEG power spectra were computed for consecutive 2 s epochs in the frequency range 1 to 50 Hz by fast Fourier transformation with a frequency resolution of 0.5 Hz. Before fast Fourier transformation, a window weighting function (Hanning) was applied. Epochs with movement-induced and other artefacts were discarded on the basis of the polygraph records. Data were presented in 1 Hz bins, and the bins were marked by their upper limits (Kantor *et al.*, 2005). The values of consecutive 2 s EEG epochs in wake, non-REM and REM sleep, respectively, were averaged over 24 h as no remarkable differences were found between power density values obtained during dark and light periods.

All results are expressed as means ± SEM. To compare vigilance state parameters, we used two-way ANOVA with repeated measures and Bonferroni test for *post hoc* comparisons (GraphPad Prism, GraphPad Software). The results were considered statistically significant at $P < 0.05$.

Results

Huntington's disease mice progressively lose their diurnal variation in sleep–wake behaviour

With increasing age, the percentage of wake in R6/2 mice gradually decreased, while both non-REM and REM sleep increased during the dark period. As a result, R6/2 mice gradually lost the normal diurnal variation in their sleep/wake behaviour (Fig. 1). When we compared the hourly amounts of wake and non-REM sleep, we found significant time × genotype (R6/2 and wild-type mice) interactions as early as 9–10 weeks of age [$F(23,299) = 1.91$, $P < 0.01$ and $F(23,299) = 2.30$, $P < 0.01$, respectively; Fig. 1]. As the disease progressed in R6/2 mice, the total amount of wake during the dark period was reduced by a further 35% at 13–14 weeks, and by 25% at 17–18 weeks of age compared with wild-type mice [time × genotype interaction: $F(2,26) = 3.79$, $P < 0.05$; Fig. 2]. This reduction in total wake amount was first due to the shortening of wake bouts as the number of wake bouts increased in R6/2 mice. In R6/2 mice, the mean duration of wake bouts was reduced by 58% at 13–14 weeks, and by 66% at 17–18 weeks of age compared to controls [time × genotype interaction: $F(2,26) = 10.22$, $P < 0.01$; Table 1]. In addition, R6/2 mice had more than twice as many wake bouts as did wild-type mice by 17–18 weeks of age during both dark and light periods [*F*-test: $F(9,4) = 24.20$, $P < 0.01$ and $F(9,4) = 77.61$, $P < 0.01$, respectively; Table 1]. This indicated a highly fragmented sleep–wake behaviour in Huntington's disease mice at the late stage of the disease.

Huntington's disease mice cannot sustain long periods of wakefulness

To understand better the inability of Huntington's disease mice to maintain wakefulness, we analysed wake as a function of bout length. During the dark period, wakefulness in mice typically occurs in very long bouts. But as the disease progressed, R6/2 mice spent less and less time in long wake bouts and instead most of the wake occurred in mid-length bouts (Fig. 3B and C). Specifically, in wild-type mice, at least 20% of wake occurred in bouts lasting over 2550 s (42.5 min), irrespective of their age. By contrast, even at the youngest age, R6/2 mice never spent more than 8% of their wake in such long bouts. By 17–18 weeks of age, 65% of wake occurred in bouts lasting >1280 s (21.2 min) in wild-type mice, whereas in R6/2 mice only 13% of wake occurred in bouts this long [bout duration × genotype interaction: $F(7,91) = 9.95$, $P < 0.01$; Fig. 3]. This demonstrated a profound deterioration of wake maintenance in Huntington's disease mice as disease progressed.

Huntington's disease mice have an increased propensity for rapid eye movement sleep

In parallel with the loss of wakefulness, the total amount of REM sleep significantly increased in R6/2 mice during the dark period. This was already evident in the first recording period at presymptomatic stage (9–10 weeks, Fig. 2). At 13–14 weeks, R6/2 mice had more than twice as much REM sleep as did wild-type mice during the dark period (Fig. 2). At the late stage of the disease, REM sleep was still elevated in R6/2 mice though to a lesser extent [time × genotype interaction: $F(2,26) = 4.74$, $P < 0.05$; Fig. 2].

To identify factors that contributed to the increase in REM sleep in R6/2 mice, we examined REM sleep architecture in detail. As the R6/2 mice became symptomatic (at 13–14 weeks), we found that they were more likely to transition into REM sleep than were wild-type mice. In wild-type mice, the probability of entering REM sleep in both light and dark period gradually increased across the duration of non-REM sleep. By contrast, by 13–14 weeks of age, R6/2 mice had a much higher probability of entering REM sleep at any time during a non-REM sleep episode if that was longer than 180 s [bout duration × genotype interactions: $F(6,78) = 4.34$, $P < 0.01$ and $F(6,78) = 6.97$, $P < 0.01$, for dark and light period, respectively; Fig. 4]. Interestingly, by late stage of the disease (17–18 weeks of age), when R6/2 mice had highly fragmented sleep–wake behaviour, the probability of entering REM sleep had returned to relatively normal levels. That is probably because they were more likely to transition into wake than REM sleep.

R6/2 mice produced more bouts of REM sleep during the dark period. R6/2 mice had at least 55% more REM sleep bouts then wild-type littermates at any stages of the disease [genotype: $F(1,13) = 23.00$, $P < 0.01$; Table 1]. In contrast, the mean duration of REM sleep bouts appeared to be similar in wild-type and R6/2 mice [genotype: $F(1,13) = 1.97$, $P = 0.18$; Table 1].

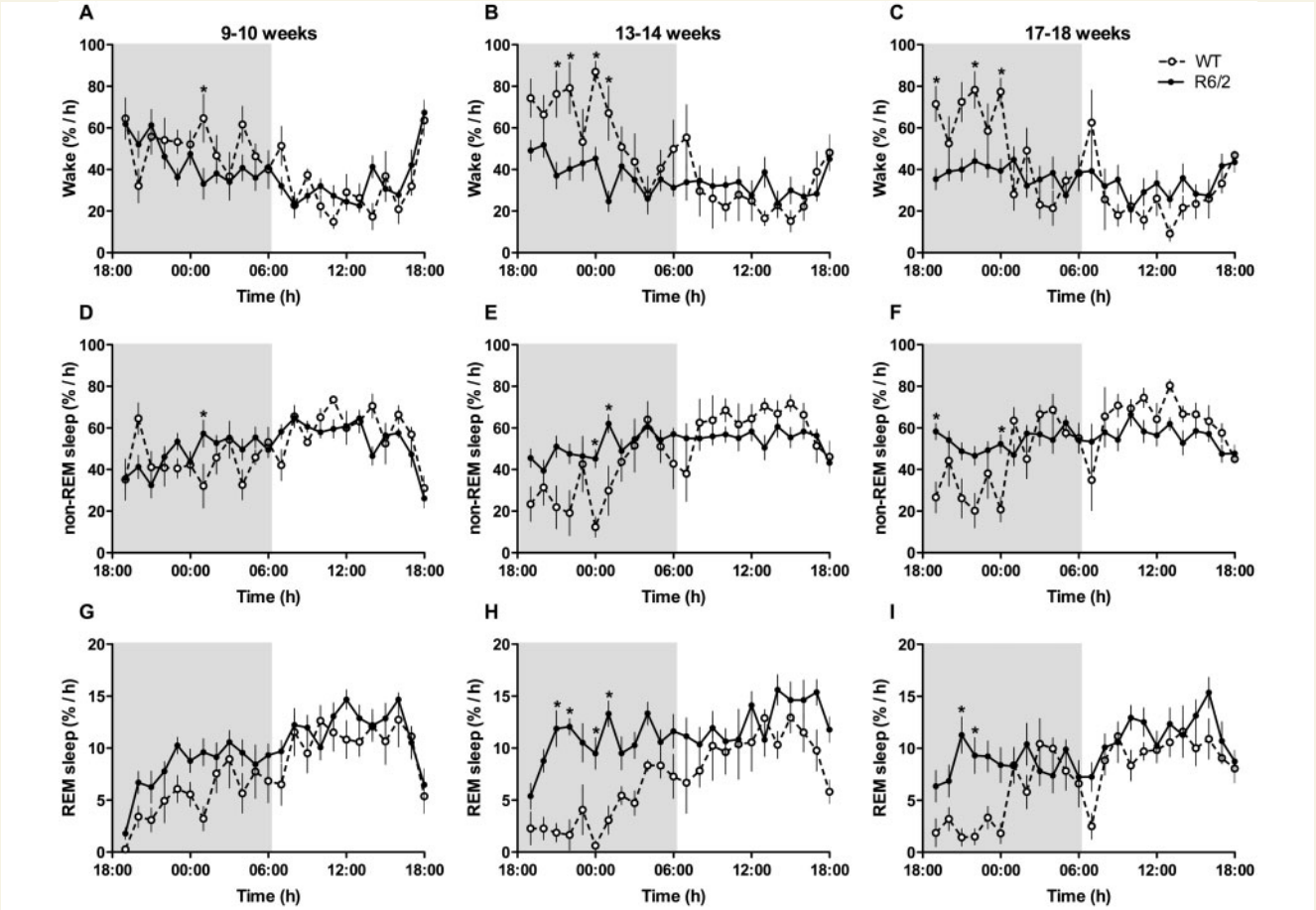

Figure 1 Normal diurnal variations in sleep/wake states in R6/2 mice were lost progressively with age. The diurnal pattern of wake (**A–C**), non-REM (NREM) sleep (**D–F**), and REM sleep (**G–I**) is shown in wild-type (WT, open symbols) and R6/2 (closed symbols) mice at presymptomatic (9–10 weeks of age; **A**, **D**, **G**), symptomatic (13–14 weeks; **B**, **E**, **H**), and late stages (17–18 weeks; **C**, **F**, **I**) of the disease. The dark period is shown as shaded area. Data are presented as mean ± SEM in 1 h intervals. $^*P < 0.05$ compared with wild-type mice (Bonferroni post-test).

Together, these data show that an increased propensity for REM sleep, demonstrated by higher probability of entering REM sleep and increased number of REM sleep bouts, resulted in an increase in REM sleep amount in R6/2 mice during the dark period. Nevertheless, while the initiation of REM sleep is seriously affected in R6/2 mice, the maintenance of REM sleep seems to be normal as shown by the normal duration of REM sleep bouts.

Huntington's disease mice develope severe abnormalities in their sleep electroencephalogram

In addition to the standard scoring, we performed a spectral analysis of the sleep EEG by means of fast Fourier transformation. This procedure allows a much more sensitive and detailed description of EEG changes than the conventional staging.

Besides alterations in sleep–wake architecture, we found that R6/2 mice also showed profound changes in their sleep EEG. In the frontoparietal region, the peak frequency of REM sleep theta rhythm in wild-type mice was invariantly at 7 Hz (Fig. 5). In contrast, the theta peak frequency in R6/2 mice gradually shifted from 7 Hz to 6 Hz as their disease progressed (Fig. 5A–C insets). The difference in REM sleep EEG between wild-type and R6/2 mice was already significant by 9–10 weeks of age when no overt symptoms were present in R6/2 mice [frequency × genotype interaction: $F(49,637) = 1.51$, $P < 0.05$; Fig. 5A]. The slowdown of theta rhythm in the frontoparietal region became more prominent once R6/2 mice started to show symptoms, namely at 13–14 weeks and 17–18 weeks of age [frequency × genotype interactions: $F(49,637) = 6.41$, $P < 0.01$ and $F(49,637) = 7.31$, $P < 0.01$, respectively; Fig. 5B and C].

In addition to the changes in REM sleep theta, R6/2 mice showed a gradual decrease in EEG slow waves during non-REM sleep in parallel with the progression of the disease. These changes were evident from both frontoparietal and frontofrontal EEG recordings (Figs 6 and 7). In the frontoparietal region, the decrease in EEG power in R6/2 mice was restricted mainly to delta frequencies (1–6 Hz) but in the frontal region it was extended up to 16 Hz. This was particularly noticeable after the mice became symptomatic. During REM sleep, we found a similar decrease in the 1–12 Hz range in the frontal region in R6/2 mice (Fig. 8).

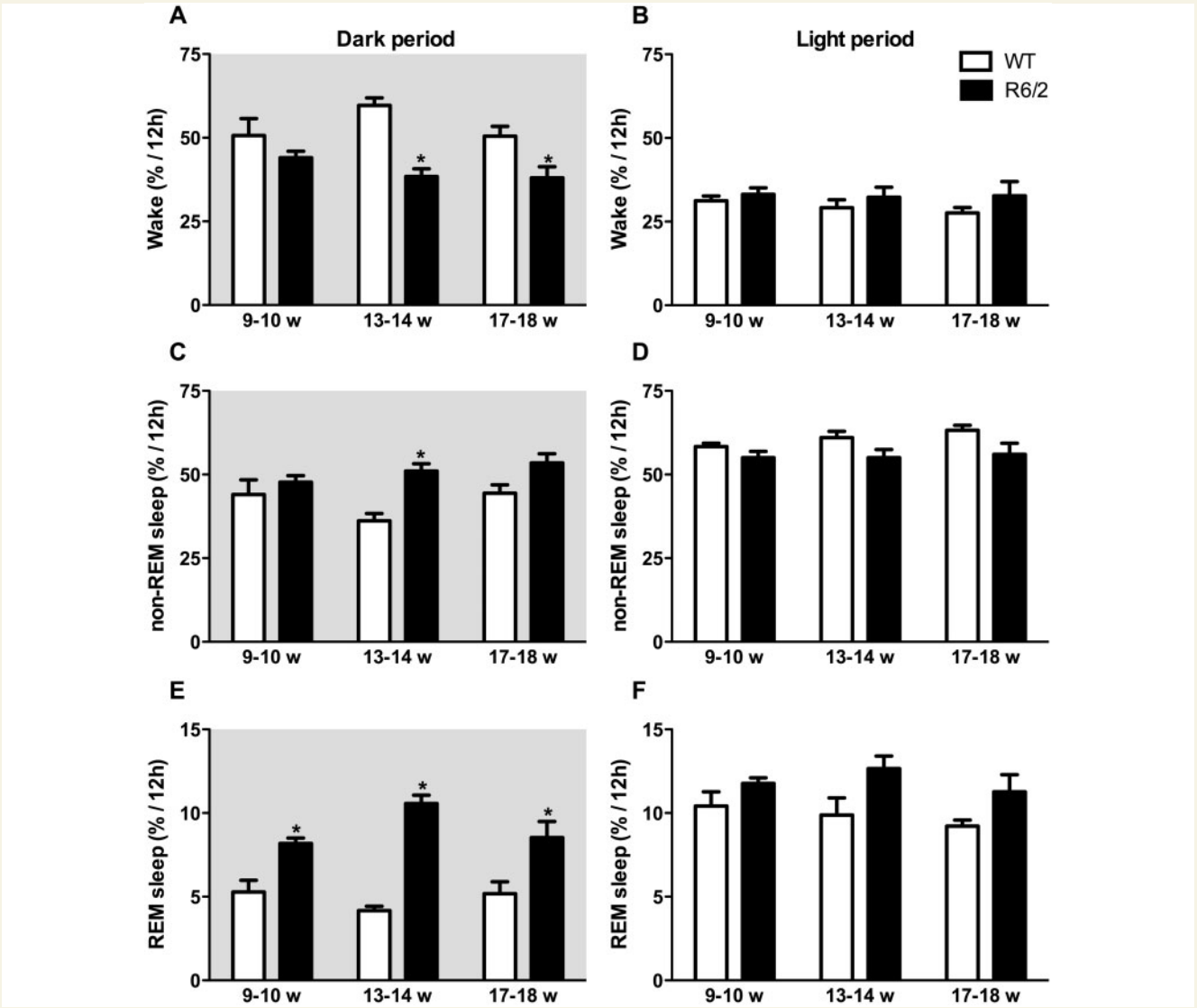

Figure 2 R6/2 mice showed a progressive decrease in the amount of wakefulness with a parallel increase in non-REM (NREM) and REM sleep amount during the dark period. Changes in the percentage of wake (**A** and **B**), non-REM sleep (**C** and **D**), and REM sleep (**E**, **F**) is shown in wild-type (WT, open bars) and R6/2 mice (closed bars) during the dark (**A**, **C** and **E**; shaded area) and light period (**B**, **D** and **F**) at presymptomatic (9–10 weeks of age), symptomatic (13–14 weeks), and late stages (17–18 weeks) of the disease. Data are presented as mean ± SEM in 12 h intervals. *$P < 0.05$ compared with wild-type mice (Bonferroni post-test).

The EEG power in low frequency ranges is several magnitudes higher than it is at high frequencies. Thus to reveal the differences between the groups in higher frequency bands, we normalized the EEG power spectral values of R6/2 mice to the mean power spectral values of age-matched wild-type mice. Compared with wild-type mice, R6/2 mice showed a gradual increase in gamma frequencies (30–40 Hz) across the frontoparietal region irrespective of sleep states (Figs 5 and 6). At the late stage of the disease (17–18 weeks), R6/2 mice had a 2-fold increase in EEG gamma activity, with a peak frequency at 32–34 Hz during both REM and non-REM sleep [frequency × genotype interactions: $F(49,637) = 14.76$, $P < 0.01$ and $F(49,637) = 14.23$, $P < 0.01$, respectively; Figs 5F and 6F]. A similar trend can be seen over the frontal region. Note that because in R6/2 mice the entire EEG spectrum is shifted down compared to that of wild-type mice [frequency × genotype interactions: $F(49,637) = 2.52$, $P < 0.01$ and $F(49,637) = 4.73$, $P < 0.01$, for non-REM and REM sleep, respectively], the values in the gamma range are overlapping in the power density spectra of the frontal region (Figs 7F and 8F).

Discussion

We found that sleep and EEG are significantly disrupted in R6/2 mice, and that these changes were observed at the earliest (presymptomatic) stage of the disease that we measured. Specifically, we found that R6/2 mice progressively lost their normal diurnal variation in sleep/wake behaviour. This was due to a progressive

Table 1 Vigilance state parameters in R6/2 mice at presymptomatic (9–10 weeks), symptomatic (13–14 weeks), and late stage (17–18 weeks) of the disease and in age matched wild-type littermates

	Wild-type ($n = 5$)			R6/2 ($n = 10$)		
	9–10 weeks	13–14 weeks	17–18 weeks	9–10 weeks	13–14 weeks	17–18 weeks
WAKE						
Mean duration (s)						
Dark period	143.20 ± 23.11	257.80 ± 58.35	237.20 ± 53.89	147.50 ± 22.56	108.40 ± 10.99*	81.00 ± 9.20*
Light period	98.80 ± 16.05	115.60 ± 7.43	115.00 ± 11.07	106.30 ± 12.55	86.80 ± 10.30	82.50 ± 10.69
Number of bouts						
Dark period	172.80 ± 34.25	126.00 ± 31.86	104.00 ± 15.40	151.00 ± 21.74	167.70 ± 20.37	245.50 ± 53.56#
Light period	155.60 ± 32.59	108.80 ± 6.41	105.40 ± 7.20	141.90 ± 11.78	187.00 ± 37.95	199.90 ± 44.86#
Non-REM SLEEP						
Mean duration (s)						
Dark period	31.00 ± 3.02	27.40 ± 1.78	36.80 ± 4.60	35.70 ± 3.39	33.50 ± 1.21	32.60 ± 3.61
Light period	36.60 ± 3.17	39.40 ± 6.24	41.40 ± 7.17	36.40 ± 2.97	34.00 ± 1.58	33.00 ± 2.79
Number of bouts						
Dark period	613.80 ± 61.71	563.60 ± 51.26	539.40 ± 67.40	650.20 ± 84.68	660.00 ± 44.89	742.90 ± 65.73
Light period	691.40 ± 50.92	735.80 ± 125.48	748.00 ± 139.73	705.00 ± 74.11	701.30 ± 48.79	771.70 ± 81.02
REM sleep						
Mean duration (s)						
Dark period	30.20 ± 2.01	27.00 ± 3.69	31.20 ± 3.88	36.90 ± 3.78	29.80 ± 0.94	37.40 ± 2.84
Light period	34.00 ± 3.05	33.20 ± 2.11	38.40 ± 5.05	34.90 ± 3.82	29.50 ± 1.39	35.30 ± 2.44
Number of bouts						
Dark period	74.40 ± 8.38	69.00 ± 6.47	73.20 ± 10.38	96.20 ± 11.54	151.30 ± 7.40*	103.20 ± 15.13
Light period	133.60 ± 14.88	129.60 ± 16.13	109.40 ± 14.35	156.70 ± 21.32	184.50 ± 11.92	141.10 ± 16.41

Mean duration, and number of bouts in each state during the dark (active) and light (passive) period. Results shown as mean ± SEM. $P < 0.05$ compared with control wild-type mice of the same age (*Bonferroni post-test and #*F*-test).

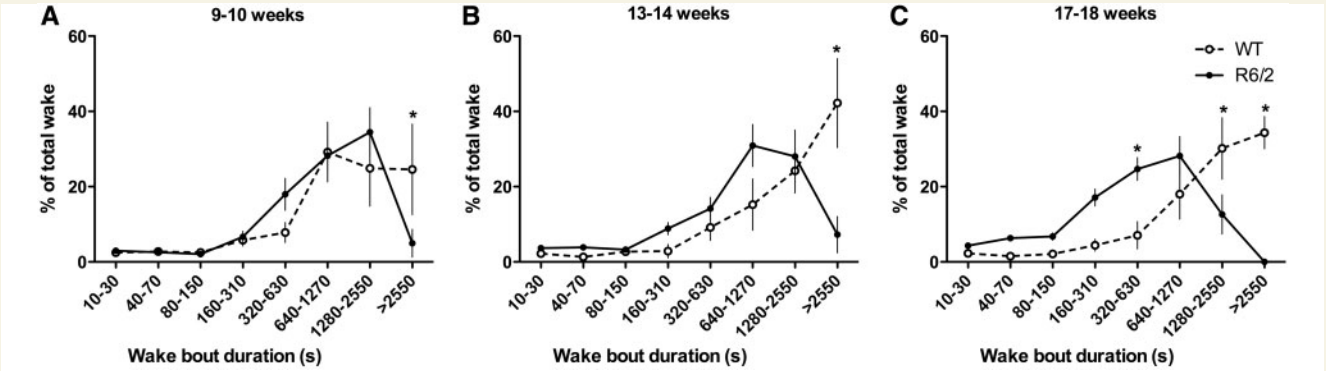

Figure 3 R6/2 mice could not sustain long periods of wakefulness. Time-weighted frequency histograms of wake bouts during the dark period as shown in wild-type (WT, open symbols) and R6/2 (closed symbols) mice at presymptomatic (9–10 weeks of age; **A**), symptomatic (13–14 weeks; **B**), and late stages (17–18 weeks; **C**) of the disease. We separated all wake bouts into one of eight bins according to length (< 30, 40–70, 80–150, 160–310, 320–630, 640–1270, 1280–2550 and > 2560 s). The percentage of wake occurring in each bin was measured and presented in a time-weighted frequency histogram as group mean ± SEM. *$P < 0.05$ compared to wild-type mice (Bonferroni post-test).

decrease in wake amount and an increase in non-REM and REM sleep amount during the dark period. As they aged, R6/2 mice had less wake during the dark period, because they gradually lost their ability to maintain long periods of wakefulness. Furthermore, the propensity for REM sleep increased dramatically in R6/2 mice with age, as shown by an increase in the number of REM sleep bouts and a higher probability of entering REM sleep. Compared with wild-type mice, the total amount of REM sleep during the dark period was doubled in R6/2 mice at the symptomatic stages of the disease. In addition to the changes in sleep–wake architecture of R6/2 mice, we found considerable alterations in their sleep EEG as the disease progressed. In particular, the peak frequency of theta rhythm during REM sleep was shifted from 7 Hz to 6 Hz, EEG slow wave activity gradually decreased during non-REM sleep, while EEG gamma activity (30–40 Hz) gradually increased during both non-REM and REM sleep in R6/2 mice. These

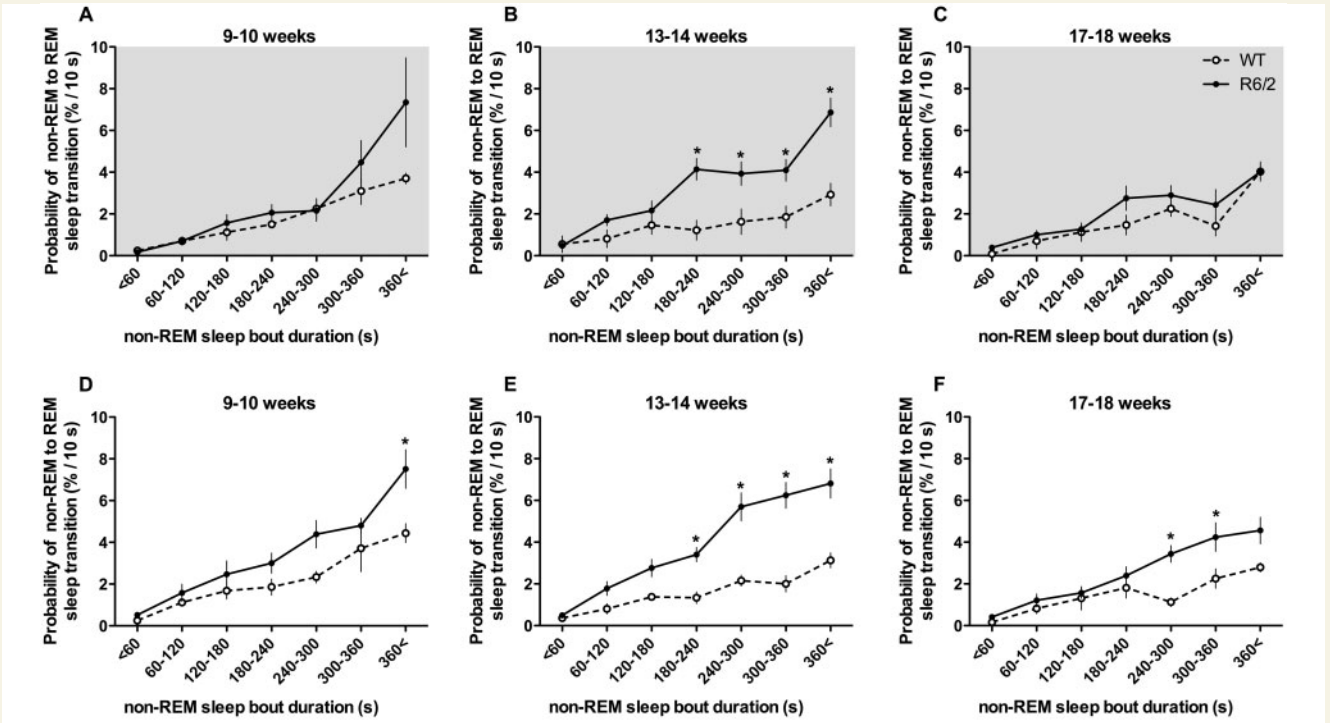

Figure 4 Symptomatic R6/2 mice had an increased probability of entering into REM sleep from a non-REM sleep episode. The probability of transitioning into REM sleep as a function of non-REM sleep bout length as shown in wild-type (open symbols) and R6/2 (closed symbols) mice during the dark (**A**–**C**) and light (**E**–**G**) period at presymptomatic (9–10 weeks of age; **A**, **D**), symptomatic (13–14 weeks; **B**, **E**), and late stages (17–18 weeks; **C**, **F**) of the disease. The absolute probability of transitioning from non-REM into REM sleep for each 10 s epoch of non-REM sleep was calculated and then the weighted average probability for bins of increasing duration ($<$90, 90–180, 180–270, 270–360 and $>$360 s) was presented as group mean $\pm$ SEM. *$P < 0.05$ compared with wild-type mice (Bonferroni post-test).

observations provide strong evidence for the presence of serious, progressive sleep and EEG abnormalities in R6/2 mice.

In our study, R6/2 mice showed a gradual decrease in wake with a concomitant increase in both non-REM and REM sleep percentage during the dark (active) period as the disease progressed. Symptomatic R6/2 mice had a highly fragmented sleep–wake behaviour shown by increased number of awakenings and shorter wake bouts. Moreover, non-REM sleep became shallow in these mice during the light (rest) period, as shown by a large reduction in slow wave activity during this stage. Our results are in accord with previously published clinical data showing that patients with Huntington's disease have a tendency for an increased daytime somnolence (Videnovic *et al.*, 2009; Goodman *et al.*, 2010), fragmented sleep–wake behaviour (Goodman *et al.*, 2011), reduced sleep efficiency, and increased stage 1 sleep during the night (Arnulf *et al.*, 2008).

Changes in REM sleep has been reported previously in patients with Huntington's disease, but these results are somewhat inconsistent. For example, Wiegand *et al.* (1991*a*, *b*) found no differences between patients with Huntington's disease and controls in any of the REM sleep parameters measured, yet in a subsequent study, polygraphic recordings were made in six patients with Huntington's disease, and reduced REM sleep was found (Silvestri *et al.*, 1995). In a more recent study, in which both medicated and unmedicated patients were included, delayed and shortened REM sleep was found in patients with Huntington's disease during the night (Arnulf *et al.*, 2008). We found no changes in REM sleep in symptomatic R6/2 mice during the rest period, but found doubled amount of REM sleep during the active period. REM sleep is clearly under strong circadian and homeostatic control (Carskadon and Dement, 1977; Beersma *et al.*, 1990; Benington and Heller, 1994; Dantz *et al.*, 1994; Dijk and Czeisler, 1995; Endo *et al.*, 1997; Wurts and Edgar, 2000; Shea *et al.*, 2008) and both Huntington's disease patients and Huntington's disease mice have disrupted circadian rhythms (Morton *et al.*, 2005). We think that an increased REM sleep during the active period may be a consequence of the disrupted circadian regulation, and that this is more apparent in the mouse (that is a species where sleep occurs anytime during a 24 h period).

As is seen in R6/2 mice, orexin-deficient mice and rats also show an increase in their REM sleep amount during the active period (Chemelli *et al.*, 1999, Hara *et al.*, 2001; Beuckmann *et al.*, 2004; Zhang *et al.*, 2007*a*, *b*; Kantor *et al.*, 2009). It has been proposed that circadian regulation of REM sleep is achieved, at least in part, by suppression of REM sleep during the active period by the orexin neurons (Kantor *et al.*, 2009). Although R6/2 mice have a functional orexin system, its circadian activity profile is disrupted and no longer follows that of the suprachiasmatic nuclei (Williams *et al.*, 2011). Therefore, one possibility would be that the incomplete suppression of REM sleep during the active period in R6/2 mice may be a result of an abnormally functioning orexin system.

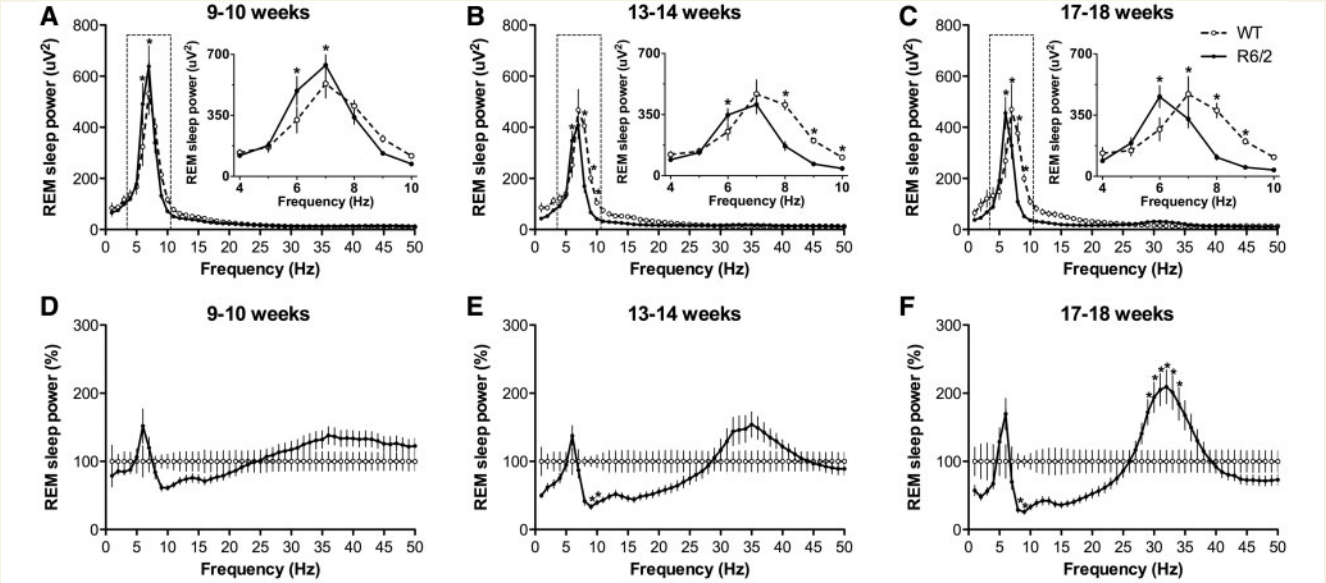

Figure 5 In R6/2 mice, theta rhythm slowed down whereas gamma activity (30–40 Hz) increased progressively in the frontoparietal region during REM sleep. Changes in absolute (**A**–**C**) and relative (**D**–**F**) power values of EEG spectra in the frontoparietal region during REM sleep as shown in wild-type (WT, open symbols) and R6/2 (closed symbols) mice during a 24 h period at pre-symptomatic (9–10 weeks of age; **A**, **D**), symptomatic (13–14 weeks; **B**, **E**), and late stages (17–18 weeks; **C**, **F**) of the disease. Enlarged images of absolute EEG power values in the theta band (framed with broken line) are shown in the insets (**A**–**C**). The EEG power spectral values of R6/2 mice were normalized to mean power spectral values (100%) of age matched wild-type mice (**D**–**F**). Data are shown as mean ± SEM in 1 Hz bins. $*P < 0.05$ compared with wild-type mice (Bonferroni post-test).

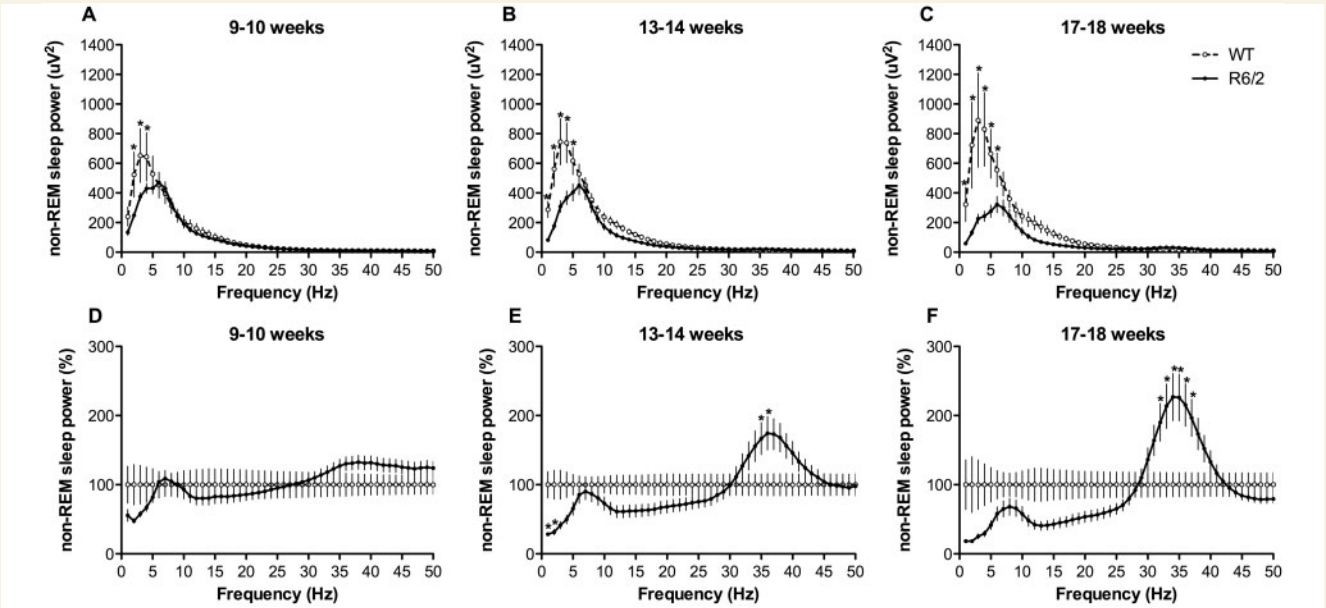

Figure 6 During non-REM sleep, EEG slow wave activity (1–6 Hz) decreased and gamma activity (30–40 Hz) increased in R6/2 mice in the frontoparietal region. Changes in absolute (**A**–**C**) and relative (**D**–**F**) power values of EEG spectra in the frontoparietal region during non-REM sleep as shown in wild-type (WT, open symbols) and R6/2 (closed symbols) mice during a 24 h period at presymptomatic (9–10 weeks of age; **A**, **D**), symptomatic (13–14 weeks; **B**, **E**), and late stages (17–18 weeks; **C**, **F**) of the disease. The EEG power spectral values of R6/2 mice were normalized to mean power spectral values (100%) of age matched wild-type mice (**D**–**F**). Data are shown as mean ± SEM in 1 Hz bins. $*P < 0.05$ compared with wild-type mice (Bonferroni post-test).

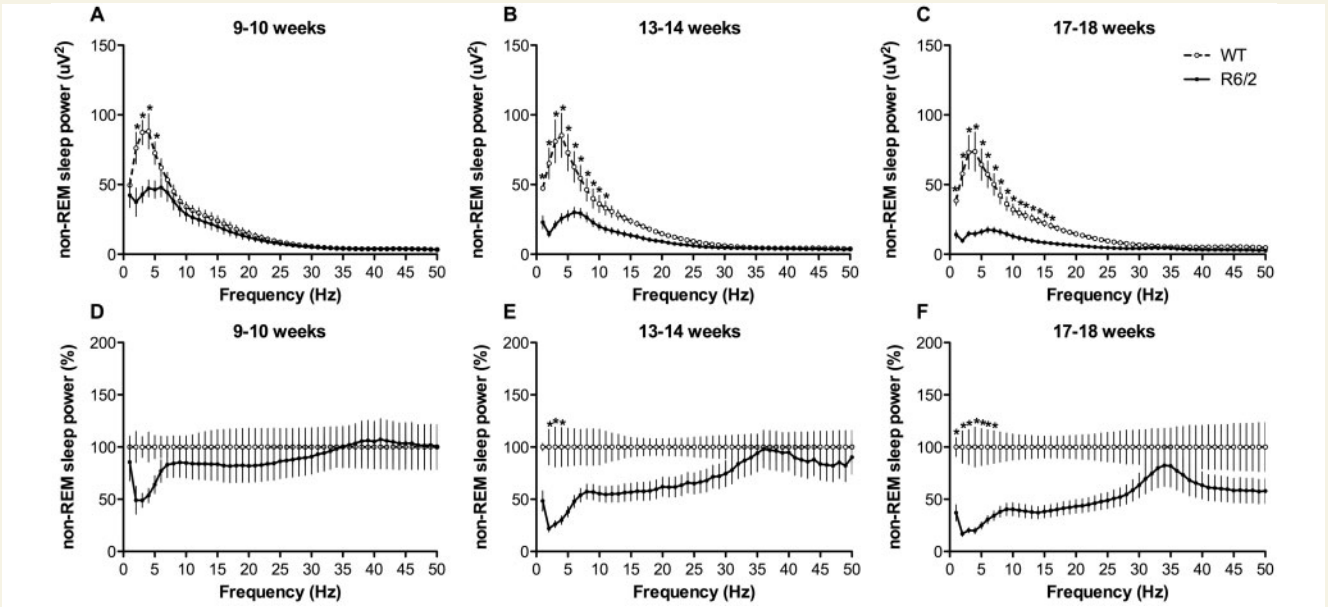

Figure 7 The power spectrum of the EEG decreased progressively in the frontal region of R6/2 mice during non-REM sleep. Changes in absolute (**A**–**C**) and relative (**D**–**F**) power values of EEG spectra in the frontal region during non-REM sleep as shown in wild-type (WT, open symbols) and R6/2 (closed symbols) mice during a 24 h period at presymptomatic (9–10 weeks of age; **A**, **D**), symptomatic (13–14 weeks; **B**, **E**), and late stages (17–18 weeks; **C**, **F**) of the disease. The EEG power spectral values of R6/2 mice were normalized to mean power spectral values (100%) of age matched wild-type mice (**D**–**F**). Data are shown as mean ± SEM in 1 Hz bins. $*P < 0.05$ compared with wild-type mice (Bonferroni post-test).

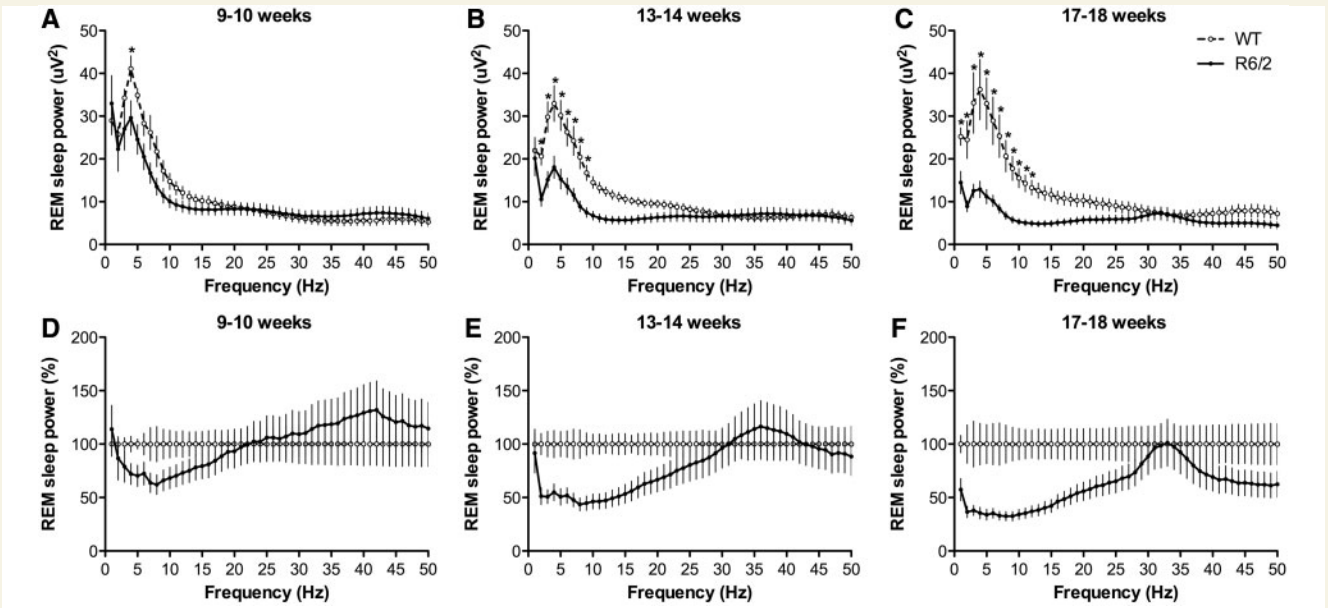

Figure 8 EEG slow wave activity (1–12 Hz) decreased progressively in the frontal region of R6/2 mice during REM sleep. Changes in absolute (**A**–**C**) and relative (**D**–**F**) power values of EEG spectra in the frontal region during REM sleep as shown in wild-type (WT, open symbols) and R6/2 (closed symbols) mice during a 24 h period at pre-symptomatic (9–10 weeks of age; **A**, **D**), symptomatic (13–14 weeks; **B**, **E**), and late stages (17–18 weeks; **C**, **F**) of the disease. The EEG power spectral values of R6/2 mice were normalized to mean power spectral values (100%) of age matched wild-type mice (**D**–**F**). Data are shown as mean ± SEM in 1 Hz bins. $*P < 0.05$ compared with wild-type mice (Bonferroni post-test).

Apart from the obvious fundamental interspecies differences, R6/2 mice lack critical genetic elements that are likely to be important in patients with Huntington's disease. R6/2 mice express only a fragment of the mutant huntingtin gene, thus the natural genomic and protein context of the polyglutamine expansion is lacking (Ehrnhoefer *et al.*, 2009). It is possible that the different genetic construct in R6/2 mice results in opposite changes in sleep in mice and patients with Huntington's disease. Although this seems unlikely, given the progressive disintegration of the sleep–wake cycle and circadian timing in R6/2 mice perfectly mirrors the circadian behavioural abnormalities observed in Huntington's disease (Morton *et al.*, 2005). Future studies will be needed to characterize fully the sleep–wake changes in patients with Huntington's disease, as well as to determine whether a full-length mutant huntingtin is necessary to fully recapitulate the symptoms of the disease in rodents.

We found that the peak frequency of theta rhythm during REM sleep was shifted gradually from 7 Hz to 6 Hz in R6/2 mice as the disease progressed. Although this may seem like a small change, theta rhythm was completely stable in wild-type mice over the 10-week recording period, and it suggests major disruption in neural activity underlying theta oscillation in R6/2 mice. A similar slow-down of theta rhythm has been shown previously in anaesthetized R6/1 mice during REM sleep (Pignatelli *et al.*, 2012) and in patients with Huntington's disease—but not normal healthy subjects—during quiet wake (Bylsma *et al.*, 1994). It has been demonstrated that the neocortical theta rhythm of rodents spreads passively from the underlying hippocampus (Gerbrandt *et al.*, 1978; Kantor *et al.*, 2005). Indeed, theta rhythmicity of field potentials recorded in most cortical areas is thought to have a septohippocampal origin (Holsheimer and Feenstra, 1977). Therefore, it seems most likely that the slowdown in neocortical theta activity that we saw is a reflection of changes in hippocampal activity. The implications of this are interesting and relevant to Huntington's disease. Hippocampal theta rhythm has been associated with learning and memory for over three decades (Berry and Thompson, 1978; Winson, 1978; Berry and Seager, 2001); and a correlation between learning and hippocampal theta has been demonstrated in both experimental animals (Buzsaki, 2002, 2005; Jones and Wilson, 2005) and humans (Caplan *et al.*, 2003; Sammer *et al.*, 2007). Moreover, it has been proposed that hippocampal oscillations during REM sleep in rodents, including theta waves, may serve for the preservation of experience-induced synaptic modifications (Buzsaki, 1998). In R6/2 mice, polyglutamine aggregates in intranuclear and extranuclear inclusions appear early in the CA1 region, and then in neurons of the CA3 field and the dentate gyrus of the hippocampus (Morton *et al.*, 2000). Abnormalities in hippocampal synaptic plasticity are already present by 3 weeks of age (Gibson *et al.*, 2005), and cognitive deficits associated with hippocampal function are measurable by 4 weeks of age (Lione *et al.*, 1999). These data, together with our results, suggest that the slow-down of theta rhythm described by us and others may be the consequence of pathophysiological changes in the hippocampus of R6/2 mice, and are likely to relate to the cognitive decline described previously in these mice.

In our study, R6/2 mice showed a progressive increase in low gamma frequency in the frontoparietal region during both non-REM and REM sleep. A similar increase in low gamma activity was found recently in the striatum of presymptomatic R6/2 mice during quiet wakefulness, which gradually disappeared as the mice increased their sensorimotor engagement with their environment (Hong *et al.*, 2012). Gamma oscillation is associated with a number of cognitive processes, including perceptual and associative learning, object representation and selective attention (Engel *et al.*, 2001; Gruber *et al.*, 2002; Fell *et al.*, 2003; Buzsaki and Draguhn, 2004). Both Huntington's disease and schizophrenic patients show abnormalities in frontostriatal pathways, perform poorly on tasks of attention and have deficits in executive functioning such as set-shifting abilities, executive planning skills, verbal fluency, verbal memory, and 'social cognition' (Sprengelmeyer *et al.*, 1996; Ho *et al.*, 2003; Snowden *et al.*, 2003; Frith, 2004; Hennenlotter *et al.*, 2004; Brune, 2005; Peinemann *et al.*, 2005; Johnson *et al.*, 2007; Allain *et al.*, 2011). Moreover, schizophrenic patients show increased gamma power during sleep and periods of psychosis (Herrmann and Demiralp, 2005). Interestingly, sub-anaesthetic doses of *N*-methyl-D-aspartate receptor antagonists that induce cognitive impairment, psychosis, hallucinations, and exacerbate symptoms in schizophrenic patients (Krystal *et al.*, 1994; Adler *et al.*, 1998; Newcomer *et al.*, 1999; Hetem *et al.*, 2000), also elicit continuous high-power gamma oscillations (30–80 Hz) lasting for hours irrespective of vigilance states (Pinault, 2008; Kittelberger *et al.*, 2012; Kocsis, 2012*a*, *b*). Therefore we speculate that the number and/or sensitivity of *N*-methyl-D-aspartate receptors are progressively changed in the striatum of patients with Huntington's disease, resulting in an altered corticostriatal communication that is accompanied by an increased gamma oscillation.

In summary, we found that sleep and sleep EEG was already disrupted in R6/2 mice by 9–10 weeks of age. These early and progressive sleep and EEG abnormalities could serve as biological markers of Huntington's disease, if they are borne out in humans. Given growing evidence that sleep and circadian changes in Huntington's disease determine the progression of the disease, these experiments may have substantial clinical relevance to people with Huntington's disease. A better understanding of the pathophysiological mechanisms underlying the disease should lead to more effective and rational therapies for Huntington's disease. An adequately treated sleep disorder could make the difference between a patient with Huntington's disease requiring 24 h versus assisted daytime care. The potential for beneficial impact on quality of life and resources is therefore considerable.

Note added in proof

Similar results in R6/2 mice have been obtained by Fisher et al., "Longitudinal analysis of the electroencephalogram and sleep phenotype in the R6/2 mouse model of Huntington's disease", Brain, in press.

Funding

This work was funded by CHDI Foundation, Inc.

References

Adler CM, Goldberg TE, Malhotra AK, Pickar D, Breier A. Effects of ketamine on thought disorder, working memory, and semantic memory in healthy volunteers. Biol Psychiatry 1998; 43: 811–16.

Allain P, Havet-Thomassin V, Verny C, Gohier B, Lancelot C, Besnard J, et al. Evidence for deficits on different components of theory of mind in Huntington's disease. Neuropsychology 2011; 25: 741–51.

Arnulf I, Nielsen J, Lohmann E, Schiefer J, Wild E, Jennum P, et al. Rapid eye movement sleep disturbances in Huntington disease. Arch Neurol 2008; 65: 482–8.

Aziz NA, Anguelova GV, Marinus J, Lammers GJ, Roos RA. Sleep and circadian rhythm alterations correlate with depression and cognitive impairment in Huntington's disease. Parkinsonism Relat Disord 2010; 16: 345–50.

Beersma DG, Dijk DJ, Blok CG, Everhardus I. REM sleep deprivation during 5 hours leads to an immediate REM sleep rebound and to suppression of non-REM sleep intensity. Electroencephalogr Clin Neurophysiol 1990; 76: 114–22.

Benington JH, Heller HC. REM-sleep timing is controlled homeostatically by accumulation of REM-sleep propensity in non-REM sleep. Am J Physiol 1994; 266: R1992–R2000.

Berry SD, Seager MA. Hippocampal theta oscillations and classical conditioning. Neurobiol Learn Mem 2001; 76: 298–313.

Berry SD, Thompson RF. Prediction of learning rate from the hippocampal electroencephalogram. Science 1978; 200: 1298–300.

Beuckmann CT, Sinton CM, Williams SC, Richardson JA, Hammer RE, Sakurai T, et al. Expression of a poly-glutamine-ataxin-3 transgene in orexin neurons induces narcolepsy-cataplexy in the rat. J Neurosci 2004; 24: 4469–77.

Bode FJ, Stephan M, Wiehager S, Nguyen HP, Bjorkqvist M, von Horsten S, et al. Increased numbers of motor activity peaks during light cycle are associated with reductions in adrenergic alpha(2)-receptor levels in a transgenic Huntington's disease rat model. Behav Brain Res 2009; 205: 175–82.

Brune M. "Theory of mind" in schizophrenia: a review of the literature. Schizophr Bull 2005; 31: 21–42.

Buzsaki G. Memory consolidation during sleep: a neurophysiological perspective. J Sleep Res 1998; 7 (Suppl 1): 17–23.

Buzsaki G. Theta oscillations in the hippocampus. Neuron 2002; 33: 325–40.

Buzsaki G. Theta rhythm of navigation: link between path integration and landmark navigation, episodic and semantic memory. Hippocampus 2005; 15: 827–40.

Buzsaki G, Draguhn A. Neuronal oscillations in cortical networks. Science 2004; 304: 1926–9.

Bylsma FW, Peyser CE, Folstein SE, Folstein MF, Ross C, Brandt J. EEG power spectra in Huntington's disease: clinical and neuropsychological correlates. Neuropsychologia 1994; 32: 137–50.

Caplan JB, Madsen JR, Schulze-Bonhage A, Aschenbrenner-Scheibe R, Newman EL, Kahana MJ. Human theta oscillations related to sensorimotor integration and spatial learning. J Neurosci 2003; 23: 4726–36.

Carskadon MA, Dement WC. Sleepiness and sleep state on a 90-min schedule. Psychophysiology 1977; 14: 127–33.

Chemelli RM, Willie JT, Sinton CM, Elmquist JK, Scammell T, Lee C, et al. Narcolepsy in orexin knockout mice: molecular genetics of sleep regulation. Cell 1999; 98: 437–51.

Dantz B, Edgar DM, Dement WC. Circadian rhythms in narcolepsy: studies on a 90 minute day. Electroencephalogr Clin Neurophysiol 1994; 90: 24–35.

Dijk DJ, Czeisler CA. Contribution of the circadian pacemaker and the sleep homeostat to sleep propensity, sleep structure, electroencephalographic slow waves, and sleep spindle activity in humans. J Neurosci 1995; 15: 3526–38.

Ehrnhoefer DE, Butland SL, Pouladi MA, Hayden MR. Mouse models of Huntington disease: variations on a theme. Dis Model Mech 2009; 2: 123–9.

Endo T, Schwierin B, Borbely AA, Tobler I. Selective and total sleep deprivation: effect on the sleep EEG in the rat. Psychiatry Res 1997; 66: 97–110.

Engel AK, Fries P, Singer W. Dynamic predictions: oscillations and synchrony in top-down processing. Nat Rev Neurosci 2001; 2: 704–16.

Etholm L, Arabadzisz D, Lipp HP, Heggelund P. Seizure logging: a new approach to synchronized cable-free EEG and video recordings of seizure activity in mice. J Neurosci Methods 2010; 192: 254–60.

Fell J, Fernandez G, Klaver P, Elger CE, Fries P. Is synchronized neuronal gamma activity relevant for selective attention? Brain Res Brain Res Rev 2003; 42: 265–72.

Franken P, Malafosse A, Tafti M. Genetic determinants of sleep regulation in inbred mice. Sleep 1999; 22: 155–69.

Frith CD. Schizophrenia and theory of mind. Psychol Med 2004; 34: 385–9.

Gerbrandt LK, Lawrence JC, Eckardt MJ, Lloyd RL. Origin of the neocortically monitored theta rhythm in the curarized rat. Electroencephalogr Clin Neurophysiol 1978; 45: 454–67.

Gibson HE, Reim K, Brose N, Morton AJ, Jones S. A similar impairment in CA3 mossy fibre LTP in the R6/2 mouse model of Huntington's disease and in the complexin II knockout mouse. Eur J Neurosci 2005; 22: 1701–12.

Goodman AO, Morton AJ, Barker RA. Identifying sleep disturbances in Huntington's disease using a simple disease-focused questionnaire. PLoS Curr 2010; 2: RRN1189.

Goodman AO, Rogers L, Pilsworth S, McAllister CJ, Shneerson JM, Morton AJ, et al. Asymptomatic sleep abnormalities are a common early feature in patients with Huntington's disease. Curr Neurol Neurosci Rep 2011; 11: 211–7.

Gruber T, Muller MM, Keil A. Modulation of induced gamma band responses in a perceptual learning task in the human EEG. J Cogn Neurosci 2002; 14: 732–44.

Hara J, Beuckmann CT, Nambu T, Willie JT, Chemelli RM, Sinton CM, et al. Genetic ablation of orexin neurons in mice results in narcolepsy, hypophagia, and obesity. Neuron 2001; 30: 345–54.

Hennenlotter A, Schroeder U, Erhard P, Haslinger B, Stahl R, Weindl A, et al. Neural correlates associated with impaired disgust processing in pre-symptomatic Huntington's disease. Brain 2004; 127: 1446–53.

Herrmann CS, Demiralp T. Human EEG gamma oscillations in neuropsychiatric disorders. Clin Neurophysiol 2005; 116: 2719–33.

Hetem LA, Danion JM, Diemunsch P, Brandt C. Effect of a subanesthetic dose of ketamine on memory and conscious awareness in healthy volunteers. Psychopharmacology (Berl) 2000; 152: 283–8.

Ho AK, Sahakian BJ, Brown RG, Barker RA, Hodges JR, Ane MN, et al. Profile of cognitive progression in early Huntington's disease. Neurology 2003; 61: 1702–6.

Holsheimer J, Feenstra BW. Volume conduction and EEG measurements within the brain: a quantitative approach to the influence of electrical spread on the linear relationship of activity measured at different locations. Electroencephalogr Clin Neurophysiol 1977; 43: 52–8.

Hong SL, Cossyleon D, Hussain WA, Walker LJ, Barton SJ, Rebec GV. Dysfunctional behavioral modulation of corticostriatal communication in the R6/2 mouse model of Huntington's disease. PLoS One 2012; 7: e47026.

Johnson SA, Stout JC, Solomon AC, Langbehn DR, Aylward EH, Cruce CB, et al. Beyond disgust: impaired recognition of negative emotions prior to diagnosis in Huntington's disease. Brain 2007; 130: 1732–44.

Jones MW, Wilson MA. Theta rhythms coordinate hippocampal-prefrontal interactions in a spatial memory task. PLoS Biol 2005; 3: e402.

Kantor S, Jakus R, Molnar E, Gyongyosi N, Toth A, Detari L, et al. Despite similar anxiolytic potential, the 5-hydroxytryptamine 2C receptor antagonist SB-242084 [6-chloro-5-methyl-1-[2-(2-methylpyrid-3-yloxy)-pyrid-5-yl carbamoyl] indoline] and chlordiazepoxide produced differential effects on electroencephalogram power spectra. J Pharmacol Exp Ther 2005; 315: 921–30.

Kantor S, Mochizuki T, Janisiewicz AM, Clark E, Nishino S, Scammell TE. Orexin neurons are necessary for the circadian control of REM sleep. Sleep 2009; 32: 1127–34.

Kittelberger K, Hur EE, Sazegar S, Keshavan V, Kocsis B. Comparison of the effects of acute and chronic administration of ketamine on hippocampal oscillations: relevance for the NMDA receptor hypofunction model of schizophrenia. Brain Struct Funct 2012; 217: 395–409.

Kocsis B. Differential role of NR2A and NR2B subunits in N-methyl-D-aspartate receptor antagonist-induced aberrant cortical gamma oscillations. Biol Psychiatry 2012a; 71: 987–95.

Kocsis B. State-dependent increase of cortical gamma activity during REM sleep after selective blockade of NR2B subunit containing NMDA receptors. Sleep 2012b; 35: 1011–6.

Krystal JH, Karper LP, Seibyl JP, Freeman GK, Delaney R, Bremner JD, et al. Subanesthetic effects of the noncompetitive NMDA antagonist, ketamine, in humans. Psychotomimetic, perceptual, cognitive, and neuroendocrine responses. Arch Gen Psychiatry 1994; 51: 199–214.

Kudo T, Schroeder A, Loh DH, Kuljis D, Jordan MC, Roos KP, et al. Dysfunctions in circadian behavior and physiology in mouse models of Huntington's disease. Exp Neurol 2011; 228: 80–90.

Lione LA, Carter RJ, Hunt MJ, Bates GP, Morton AJ, Dunnett SB. Selective discrimination learning impairments in mice expressing the human Huntington's disease mutation. J Neurosci 1999; 19: 10428–37.

Mochizuki T, Crocker A, McCormack S, Yanagisawa M, Sakurai T, Scammell TE. Behavioral state instability in orexin knock-out mice. J Neurosci 2004; 24: 6291–300.

Morton AJ. Circadian and sleep disorder in Huntington's disease. Exp Neurol 2013; 243: 34–44.

Morton AJ, Lagan MA, Skepper JN, Dunnett SB. Progressive formation of inclusions in the striatum and hippocampus of mice transgenic for the human Huntington's disease mutation. J Neurocytol 2000; 29: 679–702.

Morton AJ, Wood NI, Hastings MH, Hurelbrink C, Barker RA, Maywood ES. Disintegration of the sleep-wake cycle and circadian timing in Huntington's disease. J Neurosci 2005; 25: 157–63.

Newcomer JW, Farber NB, Jevtovic-Todorovic V, Selke G, Melson AK, Hershey T, et al. Ketamine-induced NMDA receptor hypofunction as a model of memory impairment and psychosis. Neuropsychopharmacology 1999; 20: 106–18.

Nguyen L, Bradshaw JL, Stout JC, Croft RJ, Georgiou-Karistianis N. Electrophysiological measures as potential biomarkers in Huntington's disease: review and future directions. Brain Res Rev 2010; 64: 177–94.

Peinemann A, Schuller S, Pohl C, Jahn T, Weindl A, Kassubek J. Executive dysfunction in early stages of Huntington's disease is associated with striatal and insular atrophy: a neuropsychological and voxel-based morphometric study. J Neurol Sci 2005; 239: 11–9.

Petit D, Gagnon JF, Fantini ML, Ferini-Strambi L, Montplaisir J. Sleep and quantitative EEG in neurodegenerative disorders. J Psychosom Res 2004; 56: 487–96.

Pignatelli M, Lebreton F, Cho YH, Leinekugel X. "Ectopic" theta oscillations and interictal activity during slow-wave state in the R6/1 mouse model of Huntington's disease. Neurobiol Dis 2012; 48: 409–17.

Pinault D. N-methyl d-aspartate receptor antagonists ketamine and MK-801 induce wake-related aberrant gamma oscillations in the rat neocortex. Biol Psychiatry 2008; 63: 730–5.

Rudenko O, Tkach V, Berezin V, Bock E. Detection of early behavioral markers of Huntington's disease in R6/2 mice employing an automated social home cage. Behav Brain Res 2009; 203: 188–99.

Sammer G, Blecker C, Gebhardt H, Bischoff M, Stark R, Morgen K, et al. Relationship between regional hemodynamic activity and simultaneously recorded EEG-theta associated with mental arithmetic-induced workload. Hum Brain Mapp 2007; 28: 793–803.

Shea JL, Mochizuki T, Sagvaag V, Aspevik T, Bjorkum AA, Datta S. Rapid eye movement (REM) sleep homeostatic regulatory processes in the rat: changes in the sleep-wake stages and electroencephalographic power spectra. Brain Res 2008; 1213: 48–56.

Silvestri R, Raffaele M, De Domenico P, Tisano A, Mento G, Casella C, et al. Sleep features in Tourette's syndrome, neuroacanthocytosis and Huntington's chorea. Neurophysiol Clin 1995; 25: 66–77.

Snowden JS, Gibbons ZC, Blackshaw A, Doubleday E, Thompson J, Craufurd D, et al. Social cognition in frontotemporal dementia and Huntington's disease. Neuropsychologia 2003; 41: 688–701.

Sprengelmeyer R, Young AW, Calder AJ, Karnat A, Lange H, Homberg V, et al. Loss of disgust. Perception of faces and emotions in Huntington's disease. Brain 1996; 119: 1647–65.

Trachsel L, Tobler I, Achermann P, Borbely AA. Sleep continuity and the REM-nonREM cycle in the rat under baseline conditions and after sleep deprivation. Physiol Behav 1991; 49: 575–80.

Videnovic A, Leurgans S, Fan W, Jaglin J, Shannon KM. Daytime somnolence and nocturnal sleep disturbances in Huntington disease. Parkinsonism Relat Disord 2009; 15: 471–4.

Wiegand M, Moller AA, Lauer CJ, Stolz S, Schreiber W, Dose M, et al. Nocturnal sleep in Huntington's disease. J Neurol 1991a; 238: 203–8.

Wiegand M, Moller AA, Schreiber W, Lauer C, Krieg JC. Brain morphology and sleep EEG in patients with Huntington's disease. Eur Arch Psychiatry Clin Neurosci 1991b; 240: 148–52.

Williams RH, Morton AJ, Burdakov D. Paradoxical function of orexin/hypocretin circuits in a mouse model of Huntington's disease. Neurobiol Dis 2011; 42: 438–45.

Winson J. Loss of hippocampal theta rhythm results in spatial memory deficit in the rat. Science 1978; 201: 160–3.

Wurts SW, Edgar DM. Circadian and homeostatic control of rapid eye movement (REM) sleep: promotion of REM tendency by the suprachiasmatic nucleus. J Neurosci 2000; 20: 4300–10.

Zhang S, Lin L, Kaur S, Thankachan S, Blanco-Centurion C, Yanagisawa M, et al. The development of hypocretin (orexin) deficiency in hypocretin/ataxin-3 transgenic rats. Neuroscience 2007a; 148: 34–43.

Zhang S, Zeitzer JM, Sakurai T, Nishino S, Mignot E. Sleep/wake fragmentation disrupts metabolism in a mouse model of narcolepsy. J Physiol 2007b; 581: 649–63.